Anomalous X-Ray Yields under Surface Wave Resonance during Reflection High Energy Electron Diffraction and Adatom Site Determination

Toshiro Yamanaka* and Shozo Ino†

Graduate School of Science, The University of Tokyo, 7-3-1, Hongo, Bunkyo-ku, Tokyo 1 13, Japan

(Received 23 November 1999)

In L x-ray emissions from a Si(111)-$\sqrt{3} \times \sqrt{3}$-In surface induced by electron beam irradiation were measured as functions of the incident glancing angle. Under surface wave resonance conditions, anomalous x-ray intensities were clearly observed. Using dynamical calculations, these intensities are well explained as changes in density of the electron wave field at adatom positions. From these intensities, the adatom site was analyzed, and it was found that the T_4 model is better than the H_3 model.

PACS numbers: 68.35.Bs, 61.14.Hg, 79.20.Kz

Reflection high energy electron diffraction (RHEED) has been used extensively for surface structure analysis. The patterns and their intensity are strongly affected by dynamical scattering processes, resulting in complex features of Kikuchi patterns and rocking curves. Therefore, study of the fundamental mechanism of this diffraction is important for good use. Remarkable effects of dynamical scattering are often observed when some of the diffracted beams are excited parallel to the surface, a condition known as the surface wave resonance (SWR) condition [1–5]. Under the SWR condition, the beams are temporarily trapped in the ditch of Coulomb potential of the surface atomic plane, and they propagate along the surface for a short time before they convert to specular or other diffraction beams. The intensities of the specular and diffracted beams are significantly enhanced, and this enhancement is often used to obtain clear sharp RHEED patterns [6], clear images of reflection electron microscopy, and reflection electron holography [7].

Emission yields of Auger electrons [8], secondary electrons [9], and characteristic x rays [10] from surfaces during RHEED are also enhanced under the SWR condition, since the wave field distribution is localized on the topmost layer [11–13]. Because of interference between the incident, specular, and resonant beams, the resultant wave distribution is like numerous rods oriented in the incident azimuth, of which intervals are equal to or smaller than the lattice constant. The emission yields of Auger electrons and characteristic x rays are proportional to the wave field density at the position of atoms. Therefore, it should be possible to distinguish different adatom sites from the emission yields from adatoms if the wave densities on adatoms are different depending on their sites, as pointed out by Spence and Kim [12]. Under one beam Bragg conditions where only the specular beam is strongly excited, the features of the electron wave field are very simple, and adatom height has been quantitatively determined from the anomalous intensities of characteristic x-ray emission [electron standing wave (ESW) method] [14]. However, under the SWR condition, the diffraction mechanism becomes complex due to the dynamical effect, resulting in difficulty of explanation of experimental data, and surface structure analysis has been attempted only in a qualitative way [15].

This Letter describes anomalous characteristic x-ray emissions from a Si(111)-$\sqrt{3} \times \sqrt{3}$-In surface under SWR conditions during RHEED. The intensities were analyzed by using dynamical calculation, and excellent agreement between experimental and theoretical results were obtained. The adatom site was analyzed from these anomalous intensities, showing that the T_4 model is better than the H_3 model.

We used the RHEED-TRAXS (total reflection angle x-ray spectroscopy) technique for sensitive detection of x rays emitted from surface atoms [16]. The x rays excited by the RHEED beam were detected at a fixed grazing-takeoff angle θ_t, and the glancing angle θ_g of the RHEED beam was continuously changed [14,17], as shown by the inset in Fig. 1. In the x-ray spectrum, Si K (1.74 keV) and In L (3.4 keV) were observed on bremsstrahlung ranging from 0 to 10 keV, which is equal to the energy of incident electrons. These x rays detected at a small θ_t correspond to the evanescent waves inside the crystal in a reverse process (grazing incidence of x rays). In the latter process, the penetration depth of evanescent waves depends on the x-ray incident angle and x-ray energy. Similarly, in the present case of grazing detection, the range of detection depth depends on θ_t and x-ray energy, and therefore θ_g dependences of Si K and bremsstrahlung emitted from wide depth regions change with changes in θ_t. However, the shape of θ_g dependence of In L is not affected by θ_t, since In atoms are confined in the uppermost layer. The In L intensity becomes maximum when θ_t is set at the critical angle θ_c for total reflection of In L ($=0.6°$), but the In L intensity relative to Si K and bremsstrahlung is enhanced at lower θ_t due to cutoff of x rays from deeper regions. Thus, in the present work, θ_t was set at 0.5°, which is slightly smaller than θ_c. After θ_t was optimized, a small electron gun was rotated around the sample in ultrahigh vacuum to scan θ_g, during which time the sample and x-ray detector were fixed [14,17], because x-ray spectra change drastically with only a small change in θ_t [16].

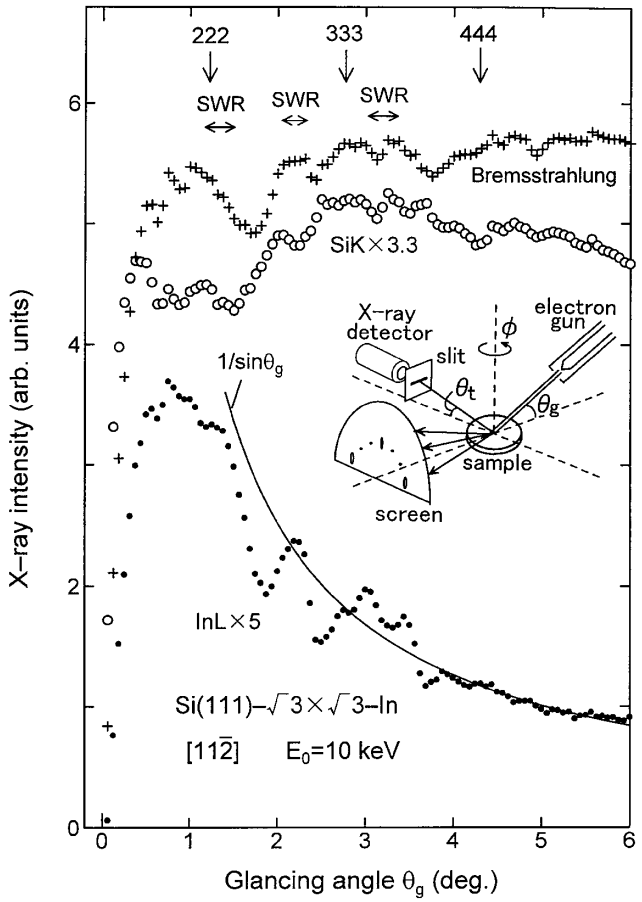

FIG. 1. θ_g dependences of In L and Si K emissions, and bremsstrahlung from a Si(111)-$\sqrt{3} \times \sqrt{3}$-In surface. The energy and incident azimuth of the primary electron beam are 10 keV and $[11\bar{2}]$, respectively. The solid line shows $1/\sin\theta_g$.

The sample was cut in a circular shape of 12 mm in diameter from a mirror-polished Si(111) wafer. The Si(111) surface was cleaned by heating up to 1200 °C by electron bombardment for about 3 sec, and the RHEED pattern showed a clear 7×7 structure. In was deposited from a coiled tungsten filament during heating of the sample at 500 °C, and a $\sqrt{3} \times \sqrt{3}$-In structure was formed.

Figure 1 shows the glancing angle (θ_g) dependence of In L, Si K, and bremsstrahlung from the $\sqrt{3} \times \sqrt{3}$-In surface. Since the sizes of the sample and beam were 12 mm and 0.12 mm, respectively, the entire beam fell on the surface at a glancing angle of more than 0.7°. However, below 0.7°, only part of the beam fell on the surface, resulting in decreased intensity. In general, In L intensities decreased almost in accordance with $1/\sin\theta_g$, which means that In atoms exist at the top layer, and the number of In atoms irradiated by the beam was proportional to $1/\sin\theta_g$ [17]. The Si K and bremsstrahlung did not show such a decrease, indicating that they were emitted from deeper regions. The In L curve showed some oscillations. The shapes of oscillations became clear when the curve was normalized by multiplying by $\sin\theta_g$, as shown in Fig. 2(a). If the θ_g dependence were expressed exactly by $1/\sin\theta_g$, the value would be constant above 0.7°. However, the measured θ_g dependence showed some inclinations, indicating that the penetration length of electrons was not sufficient. After this treatment, it became clear that the In L curve had peaks at 1.4°, 2.2°, and 2.7°–3.6°. These angles correspond to the SWR of $(1/3, 1/3$ and $-1/3, -1/3)$, $(2/3, 2/3$ and $-2/3, -2/3)$, and $(1, 1$ and $-1, -1)$, respectively. The dashed line shows θ_g dependence of x-ray emission from $\frac{1}{3}$ ML (monolayer) of In on Si substrates calculated by Monte Carlo simulation [17–19] assuming a finite sample size.

The above anomalous intensities are due to the localization of electron current density at the top layer under SWR conditions. The distribution of current density

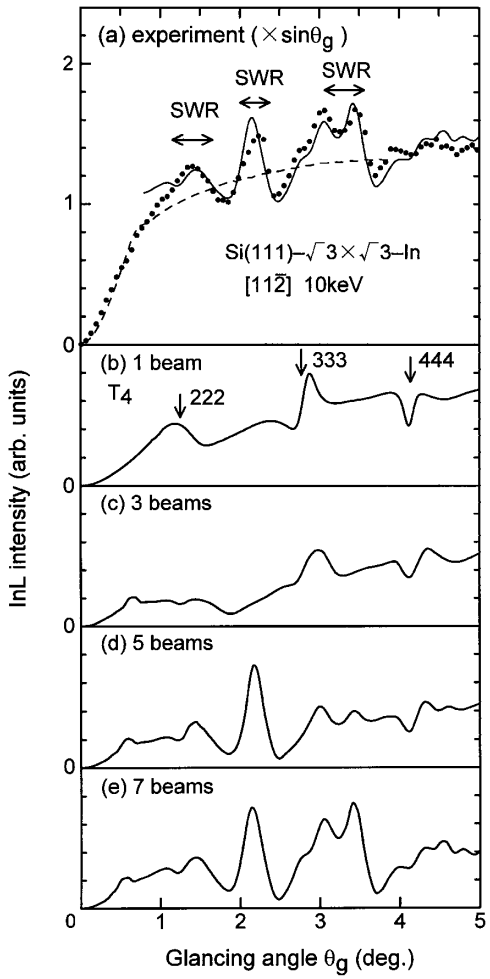

FIG. 2. (a) Normalized θ_g dependence of x-ray emission taken from Si(111)-$\sqrt{3} \times \sqrt{3}$-In, which was made from In L intensity in Fig. 1 by multiplying by $\sin\theta_g$. The dashed line shows θ_g dependences of In L from $\frac{1}{3}$ ML of In on an Si substrate calculated by Monte Carlo simulation assuming a finite size of sample. The solid line shows the theoretical curve with seven beams shown in (e). The energy and azimuth of the incident electron is 10 keV and $[11\bar{2}]$, respectively. (b)–(e) θ_g dependences of x-ray emission from a Si(111)-$\sqrt{3} \times \sqrt{3}$-In calculated by dynamical theory with one beam, three beams, five beams, and seven beams, respectively.

changes with changes in θ_g, resulting in the observed shapes of anomalous intensities. By using a dynamical theory [20,21], we calculated electron wave field densities at the positions of In in the $\sqrt{3} \times \sqrt{3}$-In as functions of θ_g, which correspond to the θ_g dependences of the x-ray emissions. Details of the methods used were described in a previous paper [14]. The T_4 adatom site [see Fig. 3(a)] was used assuming the optimum adatom height and relaxation of Si atoms determined by analysis of the RHEED rocking curve and the ESW method described in previous works [14,22]. Adsorption of In at the T_4 site has already been confirmed by several methods [22–27].

Figures 2(b)–2(e) show calculated θ_g dependences of In L emission from the $\sqrt{3} \times \sqrt{3}$-In with $[11\bar{2}]$ incidence of a 10 keV electron. Seven beams in the first Laue zone, $(1,1)$, $(2/3,2/3)$, $(1/3,1/3)$, $(0,0)$, $(-1/3,-1/3)$, $(-2/3,-2/3)$, and $(-1,-1)$, were taken into account in the calculation [see Fig. 3(b)]. When only the $(0,0)$ beam was used, the result showed anomalous intensities at Bragg angles of 222, 333, and 444 as shown in Fig. 2(b), which is similar to the result with $[21\bar{3}]$ incidence reported previously [14]. After addition of $(1/3,1/3)$ and $(-1/3,-1/3)$ beams, some structure appeared around the first SWR angle (1°–1.5°), as shown in Fig. 2(c). A new peak appeared at 2.2°, the angle of SWR of $(-2/3,2/3)$ and $(2/3,2/3)$ beams, when these two beams were added in the calculation, as shown in Fig. 2(d). When the $(1,1)$ and $(-1,-1)$ beams were added, the intensity at 2.7° to 3.6° increased, as shown in Fig. 2(e). At this stage, the calculated curve explained most of the features of the experimental curve. The addition of $(-4/3,4/3)$ and $(4/3,4/3)$ beams resulted in only small changes in the shape of the calculated curve. The above results indicate that the observed anomalous intensities are caused mainly by the SWR of these six beams in the first Laue zone.

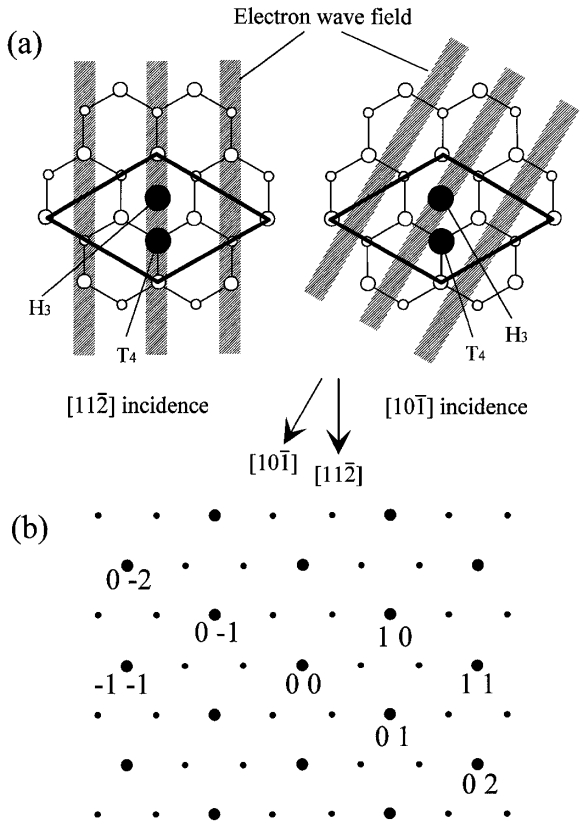

FIG. 3. (a) A schematic illustration of the T_4 and H_3 structures for Si(111)-$\sqrt{3} \times \sqrt{3}$-In, and wave field formation for the $[11\bar{2}]$ and $[10\bar{1}]$ incidence. (b) Reciprocal lattice points of the Si(111)-$\sqrt{3} \times \sqrt{3}$-In structure.

We analyzed the adatom site by comparing calculated curves for the T_4 and H_3 models with the experimental results. First, the optimum height of In assuming an H_3 structure was determined by the ESW method, analyzing the experimental result with $[21\bar{3}]$ incidence [14]. The details of this method were described in a previous paper [14]. The calculated results assuming the H_3 structure were very similar to those assuming the T_4 structure. The height of In from the ideal first Si atoms was concluded to be 1.82 Å, which is very close to the height of In determined for the T_4 structure [14,22]. Then, calculated θ_g dependences for both structures were compared with experimental results for $[11\bar{2}]$ and $[10\bar{1}]$ incidence. Figures 4(a)–4(c) show the comparison for the $[11\bar{2}]$ incidence. In the calculation, seven beams were taken into account. Both the calculated curves reproduce the features of the experimental curve. However, the shapes at angles from 0.7° to 1.5° and from 2.5° to 3.6° seem better for the T_4 structure. Figures 4(d)–4(f) show the comparison in the $[10\bar{1}]$ direction. In the calculation, seven beams, $(0,0)$, $(0,1)$, $(0,-1)$, $(0,2)$, $(0,-2)$, $(1/3,13/3)$, and $(1/3,-14/3)$, were taken into account. The calculated curves for both structures show anomalous intensities at 1.1° to 1.8° and 3.2° to 4.3°, which correspond to the SWR conditions of $(0,1)$ and $(0,-1)$, and $(0,2)$ and $(0,-2)$ beams, respectively. The SWR of $(1/3,13/3)$ and $(1/3,-14/3)$ beams occurs also around 4°. For $[10\bar{1}]$ incidence, the difference between T_4 and H_3 structures can be seen more clearly than for $[11\bar{2}]$ incidence. In the experimental curve [Fig. 4(d)], the shape of the peak at 1.1° to 1.8° is very simple, and the peak at 3.1° to 4.4° shows some shoulders with small oscillation at the lower angle side, while the slope at the higher angle side is steeper. The calculated curve for the T_4 structure in Fig. 4(e) agrees with these features. In contrast, in the theoretical curve for the H_3 structure [Fig. 4(f)], the shape at 1.1° to 1.8° is complex, and the peak at 3.1° to 4.4° shows a significant splitting at around 3.7°, resulting in poor agreement with the experimental curve. From the above comparisons, especially in $[10\bar{1}]$ incidence, we can conclude that the T_4 structure is better than the H_3 structure.

The above results showed that the $[10\bar{1}]$ incidence is more suitable for adatom site determination than is the $[11\bar{2}]$ incidence. Under SWR conditions, the wave field distribution is like numerous rods oriented in the incident azimuth, since this wave field is formed by interference between the incident, specular, and two or four SWR beams

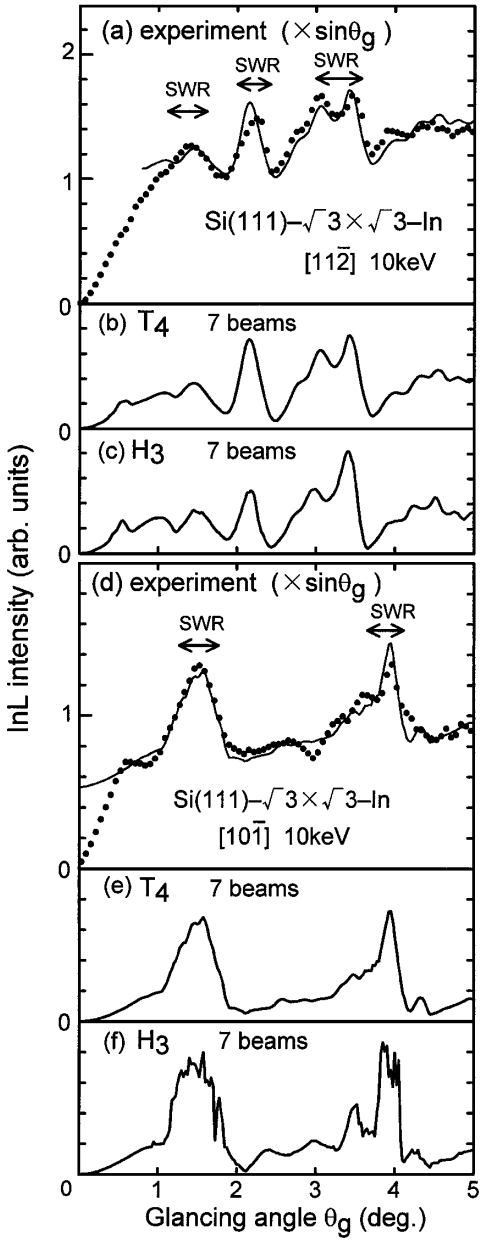

FIG. 4. (a)–(c) and (d)–(f) show comparison of experimental and theoretical curves of In L emission as functions of θ_g with $[11\bar{2}]$ incidence and $[10\bar{1}]$ incidence, respectively. (a) shows the experimental curve normalized by multiplying by $\sin\theta_g$. The solid line in (a) shows a theoretical curve for the T_4 structure shown in (b). (b) and (c) show theoretical curves for the T_4 and H_3 structures, respectively. (d)–(f) show a normalized experimental curve and theoretical curves for T_4 and H_3 structures, respectively. The solid line in (d) shows a theoretical curve for the T_4 structure shown in (e).

parallel to the surface. With the $[11\bar{2}]$ incidence, the T_4 and H_3 sites are on the same rows of the wave field, as shown in Fig. 3(a), and it is difficult to distinguish these two sites. On the contrary, with the $[10\bar{1}]$ incidence, the T_4 and H_3 sites are not on the same rows of wave field, and therefore x-ray emissions from adatoms on these two sites behave differently, and adatom sites can be easily analyzed.

*Corresponding author.
Present address: Catalysis Research Center, Hokkaido University, Sapporo 060-0811, Japan.
Email address: yama@cat.hokudai.ac.jp
†Present address: Department of Electronics, Faculty of Engineering, Utsunomiya University, Utsunomiya 321-8585, Japan.

[1] S. Kikuchi and S. Nakagawa, Sci. Pap. Inst. Phys. Chem. Res. **21**, 256 (1933).
[2] E. G. McRae, J. Chem. Phys. **45**, 3258 (1966).
[3] E. G. McRae, Rev. Mod. Phys. **51**, 541 (1979).
[4] S. Miyake and K. Hayakawa, Acta Crystallogr. Sect. A **26**, 60 (1970).
[5] Z. Mitura and P. A. Maksym, Phys. Rev. Lett. **70**, 2904 (1993).
[6] S. Ino, Jpn. J. Appl. Phys. **16**, 891 (1977).
[7] N. Osakabe, T. Matsuda, J. Endo, A. Tonomura, and A. Fukuhara, Phys. Rev. Lett. **62**, 2969 (1989).
[8] A. Ichimiya and Y. Takeuchi, Surf. Sci. **128**, 343 (1983).
[9] H. Marten, in *RHEED and Reflection Electron Imaging of Surface*, edited by P. K. Larsen and P. J. Dobson (Plenum, New York, 1987), p. 109.
[10] T. Yamanaka, Ph.D. thesis, The University of Tokyo, 1993.
[11] Z. L. Wang, Ultramicroscopy **24**, 371 (1988).
[12] J. C. H. Spence and Y. Kim, in *RHEED and Reflection Electron Imaging of Surface* (Ref. [9]), p. 117.
[13] Y. Horio, Jpn. J. Appl. Phys. **37**, L164 (1998).
[14] T. Yamanaka, T. Hanada, and S. Ino, Phys. Rev. Lett. **75**, 669 (1995).
[15] Y. Horio and A. Ichimiya, Surf. Sci. **164**, 589 (1985).
[16] S. Hasegawa, S. Ino, Y. Yamamoto, and H. Daimon, J. Appl. Phys. **24**, L387 (1985).
[17] T. Yamanaka, A. Endo, and S. Ino, Surf. Sci. **294**, 53–66 (1993).
[18] R. Shimizu, Jpn. J. Appl. Phys. **22**, 1631 (1983).
[19] D. E. Newbury, in *Advanced Scanning Electron Microscopy and X-ray Microanalysis*, edited by D. E. Newbury, D. C. Joy, P. Echlin, C. E. Fiori, and J. I. Goldstein (Plenum Publishing Corporation, New York, 1986), p. 3.
[20] A. Maksym and J. L. Beeby, Surf. Sci. **110**, 423 (1981).
[21] A. Ichimiya, Jpn. J. Appl. Phys. **22**, 176 (1983).
[22] T. Hanada, H. Daimon, and S. Ino, Phys. Rev. B **51**, 13 320 (1995).
[23] J. M. Nicholls, P. Martensson, G. V. Hansson, and J. E. Northrup, Phys. Rev. B **32**, 1333 (1985).
[24] J. C. Woicik *et al.*, Phys. Rev. Lett. **71**, 1204 (1993).
[25] J. Nogami, Sang-il Park, and C. F. Quate, J. Vac. Sci. Technol. B **6**, 1479 (1988).
[26] K. Izumi, T. Takahashi, and S. Kikuta, Jpn. J. Appl. Phys. **28**, 1742 (1989).
[27] N. Nakamura, K. Anno, and S. Kono, Surf. Sci. **262**, L101 (1992).